ANTICANCER RESEARCH *38*: 187-197 (2018)
doi:10.21873/anticanres.12207

Deregulation of Nicotinamide N-Methyltransferase and Gap Junction Protein Alpha-1 Causes Metastasis in Adenoid Cystic Carcinoma

KANA ISHIBASHI[1], KOTARO ISHII[1], GORO SUGIYAMA[1], TOMOKI SUMIDA[1], TSUYOSHI SUGIURA[2], YU KAMATA[1], KATSUHIRO SEKI[1], TAKAHIRO FUJINAGA[1], WATARU KUMAMARU[1], YOSUKE KOBAYASHI[1], NAOMI HIYAKE[1], HIROYUKI NAKANO[1], TOMOHIRO YAMADA[1] and YOSHIHIDE MORI[1]

[1]*Section of Oral & Maxillofacial Surgery, Division of Maxillofacial Diagnostic and Surgical Sciences, Faculty of Dental Science, Kyushu University, Fukuoka, Japan;*
[2]*Department of Maxillofacial Diagnostic and Surgical Science, Field of Oral and Maxillofacial Rehabilitation, Graduate School of Dental Science, Kagoshima University, Kagoshima, Japan*

Abstract. *Background/Aim: Adenoid cystic carcinoma (AdCC) is a malignant tumor that occurs in the salivary glands and frequently metastasizes. The aim of this study was to identify factors mediating AdCC metastasis. Materials and Methods: We established three AdCC cell lines by orthotropic transplantation and in vivo selection: parental, highly metastatic (ACCS-M-GFP), and lymph node metastatic (ACCS-LN-GFP) cells. Results: We examined the three cell lines. DNA microarray indicated significantly altered processes in ACCS-LN-GFP cells: particularly, the expression of nicotinamide N-methyltransferase (NNMT) was enhanced the most. NNMT is associated with tumorigenesis and is a potential tumor biomarker. Concomitantly, we found-significant down-regulation of gap junction protein alpha-1. We suggest that ACCS-LN-GFP cells acquire cancer stem cell features involving the up-regulation of NNMT and the loss of gap junction protein alpha-1, leading to epithelial–mesenchymal transition and consequent AdCC metastasis. Conclusion: NNMT is a potential biomarker of AdCC.*

Adenoid cystic carcinoma (AdCC) is a common cause of head and neck malignant tumors. AdCC is characterized by slow development, local invasion of the nerves and vessels, and distant metastases, especially in the lungs. Approximately 40-60% of AdCCs metastasize (1, 2) and the metastases are characterized by low sensitivity for chemotherapy or radiotherapy; therefore, AdCC is often difficult to treat, and associated with poor prognosis (3). Furthermore, molecular targeted therapies have not been developed to treat this disease, as it has happened for other malignant tumors (4). It is crucial to elucidate the biological characteristics of AdCC with respect to tumorigenesis and tumor metastasis. To understand the mechanism of AdCC metastasis, we have previously established two AdCC cell lines green fluorescent protein (GFP) gene transferred by injecting cells to the tongue and *in vivo* selection in nude mice: the parental ACCS-GFP and the highly metastatic ACCS-M-GFP cell lines. DNA microarray analysis was examined and the results revealed significantly altered biological molecules associated to cell adhesion and signaling in ACCS-M-GFP cells. In particular, a significant down-regulation of cell adhesion molecules such as E-cadherin and integrin and up-regulation in the expression of vimentin was observed. We concluded that the epithelial-mesenchymal transition (EMT) is the important phenomenon that cells disseminate from the primary tumor site and lead to AdCC metastasis (5).

In a different study, we confirmed a direct relation between the EMT and cancer stem-like cells (CSCs) in the highly metastatic ACCS-M-GFP cells. Furthermore, we reported that the T-box transcription factor Brachyury, which is also a marker of mesoderm differentiation, regulates CSCs and the EMT in AdCC (6). Brachyury-knockdown exerted stronger effects on cancer stemness and the EMT phenotype than the knockdown of the conventional CSCs regulator Sox2. By reducing the stemness of CSCs, Brachyury knockdown significantly inhibited tumorigenicity and metastasis *in vivo* (7).

Correspondence to: Dr. Kotaro Ishii, Section of Oral & Maxillofacial Surgery, Division of Maxillofacial Diagnostic and Surgical Sciences, Faculty of Dental Science, Kyushu University, 3-1-1, Maidashi, Higashi-ku, Fukuoka, 812-8582, Japan. Tel: +81 926426452, Fax: +81 926426392, e-mail: kishii17@dent.kyushu-u.ac.jp

Key Words: Adenoid cystic carcinoma, primary tumor cell lines, metastatic cell lines, epithelial–mesenchymal transition, nicotinamide N-methyltransferase.

In our previous studies, we used cell lines established from the primary tumor site, with high metastatic potential. However, to identify metastasis-associated molecules it is important to examine cells that have metastasized through the detachment from the tumor mass, intra- and extra-vascular invasion and tumor formation at distant sites. Therefore, in this study, we established the lymph node metastatic cell line ACCS-LN-GFP from AdCC cells, using orthotropic transplantation in nude mice. The derived lymph node metastatic and parental cell lines were then subjected to DNA microarray analysis. Data mining analysis identified uniquely expressed genes in lymph node metastatic cells, and this result was validated using ACCS cell lines. Both the computational and experimental validation highlighted the biological alterations associated with lymph node metastatic ACCS cells.

Materials and Methods

Cells and culture. The human adenoid cystic carcinoma cell lines ACCS, ACCS-GFP, and ACCS-M-GFP were established in our laboratory, as reported previously (5, 8). The parental ACCS cells and GFP-transfected ACCS (ACCS-GFP) cells displayed similar morphologies, growth rates, and tumorigenicity both *in vitro* and *in vivo*. As the parental ACCS, the tumorigenicity of the ACCS-GFP cells was low (22.2% incidence). We examined tumor formation in the tongue of nude mice injected with ACCS-GFP cells and observed, under excitation light, the fluorescence associated with the tumors. We performed *in vivo* selection of the clones with higher tumorigenicity by repeatedly recovering the tumor cells and transplanting them into the tongue of nude mice. Through this process, we obtained ACCS-M-GFP cells, a sub-line exhibiting high tumorigenicity (100% incidence) and a high frequency of spontaneous metastasis to submandibular lymph nodes (100% incidence). The histological and immunohistochemical features of ACCS-M-GFP tumors were similar to those of the solid AdCC. These cell lines were maintained as monolayer cultures in Dulbecco's modified Eagle's medium (DMEM; Sigma-Aldrich, St. Louis, MO, USA) supplemented with 10% fetal bovine serum (FBS; Filton Pty, Brooklyn, Australia), 2 mM L-glutamine (Wako Pure Chemical Industries, Osaka, Japan), penicillin G (Meiji Seika Pharma, Tokyo, Japan), and streptomycin (Meiji Seika Pharma, Tokyo, Japan) in a 5% CO_2 incubator at 37˚C. The cell lines were passaged using 0.05% trypsin/EDTA (Gibco, Grand Island, NY, USA) and phosphate-buffered saline (PBS).

Animals and ACCS-M-GFP metastatic orthotropic implantation mouse model. The animal experimental protocols were approved by the Animal Care and Use Committee of the Kyushu University, (Fukuoka, Japan). Eight-week-old female athymic nude mice (BALBcAJcl-nu) were purchased from Kyudo (Fukuoka, Japan). The mice were housed in laminar flow cabinets under specific pathogen-free conditions, in facilities approved by the Kyushu University. For the experimental metastasis studies, 1×10^6 cells in 40 μl PBS were injected into the tongue of mice under intraperitoneal diethyl ether anesthesia, using a syringe with a 27-gauge disposable needle (TOP Plastic Syringe, Tokyo, Japan). The primary tumor volumes were measured weekly, calculated as length × width × thickness, and the mice were sacrificed when the primary tumor volume reached 100 mm^3. After sacrifice, the tongue, cervical lymph nodes, lungs, and liver were observed macroscopically. The tumors and the metastasis of GFP-transfected clones were also visualized macroscopically under light excitation. After visualization, the primary tumors and metastatic sites were examined pathologically and immunohistochemically. Lymph metastatic AdCC tumors were cultured on plastic tissue culture dishes using the explant cell culture method.

Cell count and cell growth curves for the AdCC cell lines. Sub-confluent cells were observed under a fluorescence microscope (BZ-8000; Keyence, Osaka, Japan), and the cells in four fields were counted. Cell growth was evaluated counting the ACCS-GFP, ACCS-M-GFP, and ACCS-LN-GFP cells cultured on 3-cm-diameter plastic plates, every 24 h. Assays were performed in triplicate and repeated three times.

Wound healing assay. Each cell line (3×10^5 cells) was seeded on a 6-well plate, and 24 h later 'wounds' were created by scratching the plate surface with a 200-μl pipette tip. The plate was then washed with medium, and observed under a fluorescence microscope. The wound regions were photographed after 8, 16, and 24 h. The wound area was calculated using the following formula: Wound area (% of control)=Wound area at the indicated period ×100/initial wound area. All experiments were carried out in triplicate and repeated three times.

Total RNA isolation. Total RNA was isolated from ACCS-GFP, ACCS-M-GFP, and ACCS-LN-GFP cells using TRIzol Reagent (Invitrogen, Carlsbad, CA, USA) and was purified using an SV Total RNA Isolation System (Promega, Madison, WI, USA) according to the manufacturer's instructions. RNA samples were quantified with an ND-1000 spectrophotometer (Nano Drop Technologies, Wilmington, DE, USA), and their quality was confirmed with an Experion System (Bio-Rad Laboratories, Hercules, CA, USA).

Gene expression microarrays. The cRNA was amplified, labeled, and hybridized to a 60K Agilent 60-mer oligomicroarray (SurePrint G3 Human Gene Expression Microarray 8×60 K, v2; Agilent Technologies, Santa Clara, CA, USA) according to the manufacturer's instructions. All hybridized microarray slides were scanned by an Agilent scanner. Relative hybridization intensities and background hybridization values were calculated using the Agilent Feature Extraction software (9.5.1.1).

Data analysis and filter criteria. Raw signal intensities and flags for each probe were calculated from hybridization intensities (gProcessedSignal), and spot information (*e.g.*, gIsSaturated) according to the procedures recommended by Agilent. Following are the flag criteria in the GeneSpring Software: Absent (A), 'Feature is not positive and significant' and 'Feature is not above background'; Marginal (M), 'Feature is not uniform', 'Feature is saturated', and 'Feature is a population outlier'; and Present (P): others. The raw signal intensities of two samples were log2-transformed and normalized by quantile algorithm with the 'preprocessCore' library package by using the open source Bioconductor software.

We selected probes that we called the 'P' flag in both samples. To identify up- and down-regulated genes, we calculated the Z-scores and ratios (non-log scaled fold-change) from the normalized signal intensities of each probe for comparison between control and experiment samples. Then, we established the criteria for regulated genes: up-regulated genes, Z-score ≥2.0 and ratio ≥5-fold; down-regulated genes, Z-score ≤–2.0 and ratio ≤0.2. The extracted data were analyzed using DAVID, a database of the National Institute of Allergy and Infectious Diseases (NIAID). In addition, microarray data analysis was supported by Cell Innovation platform.

Quantitative PCR(qPCR). The expression of the nicotinamide N-methyltransferase (NNMT) gene in AdCC cells was quantified by qPCR. Total RNA was extracted from ACCS-M-GFP and ACCS-LN-GFP cells using an RNeasy Mini kit (Qiagen, Chatsworth, CA, USA) and used for first-strand cDNA synthesis. The mRNA levels were quantified in triplicate using a qPCR system (Roche Diagnostics, Mannheim, Germany) with the Light Cycler® Fast Start DNA Master SYBR Green I Kit (Roche Diagnostics, Mannheim, Germany). The specific NNMT primers were (F) 5'-GAGCAGAAGTTCTCCAGCCT-3' and (R) 5'-ACCATTCG ATTGTGTAGCCA-3'. Amplification was performed using the following conditions: denaturation at 95˚C for 10 min followed by 46 cycles of annealing at 60˚C for 10 sec and extension at 72˚C for 10 sec. Dissociation curve analyses confirmed that the signals corresponded to unique amplicons. Each experiment was done in triplicate, and the results were normalized against the mRNA levels of glyceraldehyde-3-phosphate dehydrogenase (*GAPDH*) obtained from parallel assays and analyzed using the LightCycler® 2.0 System software (Roche Diagnostics, Mannheim, Germany).

Western blot. Cultured cells were rinsed with PBS and then lysed by sonication in sodium dodecyl sulfate (SDS) lysis buffer (50 mM Tris-HCl [pH 6.8], 2% SDS, 10% glycerol, and 6% mercaptoethanol) containing a protease inhibitor cocktail (Sigma-Aldrich, St. Louis, MO, USA). The protein contents of the lysates and fractionated samples were quantified using the Bio-Rad Protein Assay Kit (Bio-Rad Laboratories, Hercules, CA, USA). An equal amount of protein (30 μg) from each sample was electrophoresed on 10% SDS polyacrylamide gels and transferred electrophoretically onto a nitrocellulose membrane (Bio-Rad Laboratories, Hercules, CA, USA). After washing with TBST (25 mM Tris-HCl [pH 8.2], 144 mM NaCl, and 0.1% Tween 20), the membranes were blocked with 5% non-fat skimmed milk in TBST at 20-25˚C. Immunoreactive bands were visualized using horseradish peroxidase-conjugated secondary antibodies (DAKO, Carpinteria, CA, USA) and ECL detection reagents (Amersham Pharmacia Biotech, Piscataway, NJ, USA). Bands were quantified using the Quantity One Software (Bio-Rad Laboratories, Hercules, CA, USA) after scanning by computer-assisted densitometry (ChemiDoc XRS-J; Bio-Rad Laboratories, Hercules, CA, USA). Beta-actin was used as a loading control. The primary antibodies used for immunoblotting were: mouse monoclonal antibody against NNMT (ab119758, Abcam, Cambridge, UK); and mouse monoclonal antibody against β-actin (A5316, Sigma-Aldrich, St. Louis, MO, USA).

Statistical analysis. All data are presented as mean±the standard deviation (SD), as analyzed *via* analysis of variance and Student's *t*-test, and processed using the SPSS 13.0 software (IBM, Armonk, NY, USA). Statistical significance was defined as $p<0.05$.

Results

Establishment of the lymph node metastatic cell line ACCS-LN-GFP. We previously created the ACCS-GFP cell line, upon stable GFP transfection in AdCCs (5). ACCS-GFP cells implanted in the tongue of nude mice showed low tumorigenicity and no metastasis formation. We repeatedly injected these cells in the mouse tongue and isolated the tumors that originated. As a result of this multi-step selection, we obtained ACCS-M-GFP cells, a cell line with 100% rate of metastasis. The tumor primary site and the metastatic sites (under an optic (Figure 1A, D and G) were visualized as green spots under a fluorescence microscope (Figure 1B, E and H). Histopathological examination of the primary tumor (Figure 1C) indicated that its border was unclear and that large and small cancer nests were scattered. On the other hand, the pathological examination of the cervical lymph node metastases indicated that the cancer had undergone follicular-shaped proliferation (Figure 1F). Additionally, the tongue tumors formed upon injection of ACCS-LN-GFP cells showed the solid pattern of AdCC (Figure 1I). We then successfully established the lymph node metastatic cell line from the lymph node metastatic tumors. We also attempted establishing a lung metastatic cell line with the same procedure. However, we were not successful, because the lung metastases were too small. In this study, we used the three cell lines: ACCS-GFP, ACCS-M-GFP, and ACCS-LN-GFP.

Morphology of ACCS-GFP and ACCS-LN-GFP cells. ACCS-GFP and ACCS-LN-GFP cell images were obtained using a phase-contrast microscope. ACCS-GFP cells exhibited a thin, small crescent shape, whereas ACCS-LN-GFP cells were oval, with swollen cytoplasm and nucleus (Figure 2A). The cellular formation of ACCS-M-GFP is equal to that of ACCS-LN-GFP (data not shown). Additionally, the number of ACCS-LN-GFP cells in an optical field was approximately 2.5 times lower than that of ACCS-GFP cells (Figure 2B).

Proliferation of the ACCS cell lines. The proliferative ability of the ACCS cell lines was evaluated. ACCS-GFP cells proliferated 1.2 times faster than ACCS-M-GFP or ACCS-LN-GFP cells at 6 days, at which point all cell lines reached confluency (Figure 3).

Migration of the ACCS cell lines. The migratory ability of the ACCS cell lines was examined in a wound healing assay (Figure 4). The wound area in the ACCS-GFP cell culture after 24 h from the scratch was reduced by ~50%. Notably, at the same time point, the wound areas of the ACCS-M-GFP and ACCS-LN-GFP cell cultures were ~40% and ~30% of the original ones, respectively. These data indicated that the migratory ability of the ACCS-LN-GFP cells had a

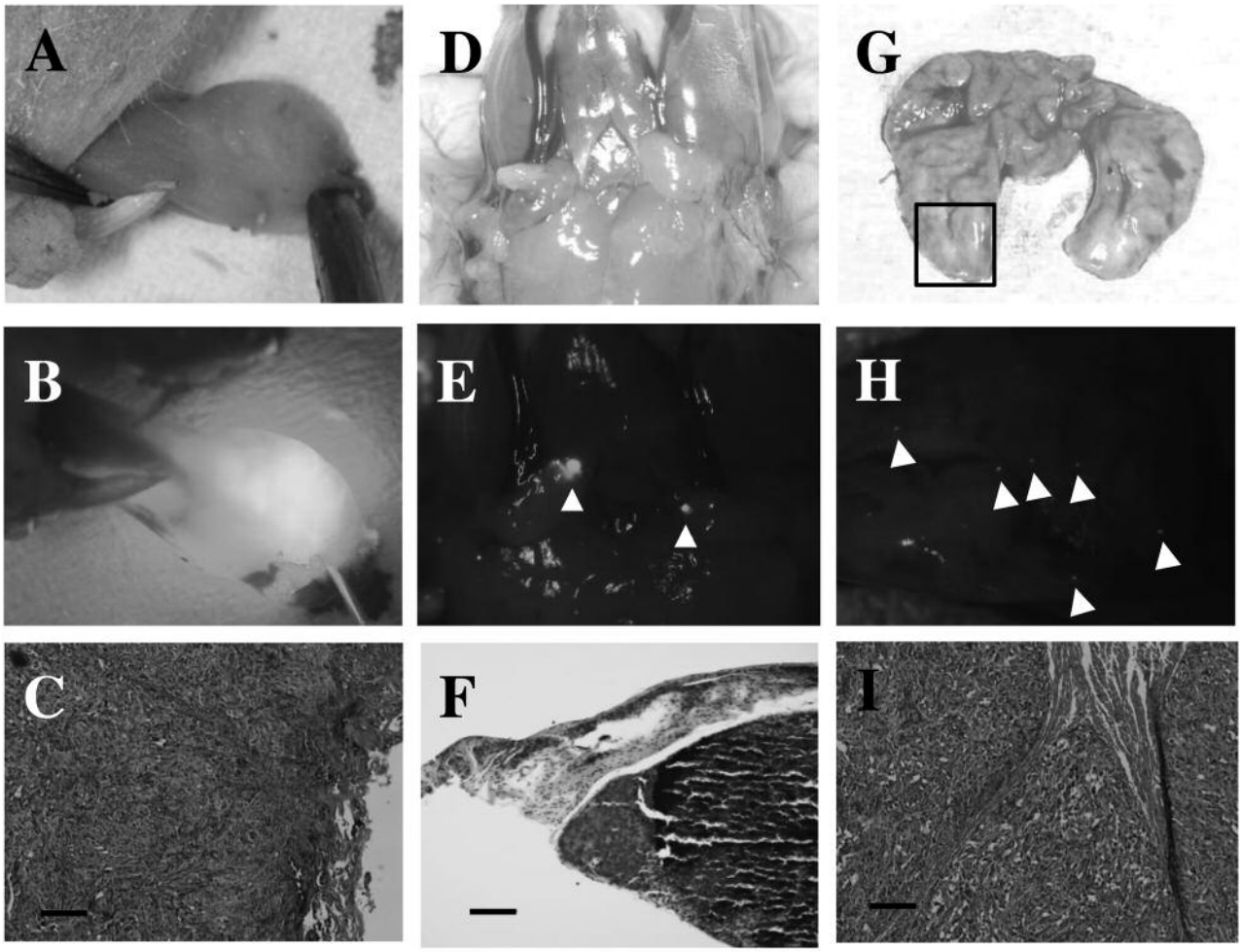

Figure 1. *Detection of tumors and metastases upon ACCS-M-GFP injection. (A and B) Tongues, (D and E) lymph nodes, and (G and H) lungs of nude mice injected with ACCS-M GFP cells were examined to detect tumors or metastases. (A, D, and G) Photographs captured under normal light and (B, E, and H) a fluorescence microscope are shown. The sites of lung metastasis are indicated by arrowheads. Micro-metastasis (GFP-positive) were observed in the lymph nodes and lungs. (C) Histopathology of primary tumors, (F) metastatic lymph nodes, and (I) tumor detected after ACCS-LN-GFP cells were injected into mouse tongue. After the mice were sacrificed, the tongue and the metastatic lymph nodes were removed and fixed with 2% paraformaldehyde in PBS. Paraffin-embedded tissue sections (5-μm thickness) were stained with hematoxylin and eosin. Scale bars indicate 100 μm.*

tendency of the increment compared to ACCS-GFP cells. However, there was no significant difference among them.

Microarray analysis. We previously reported the microarray analysis of ACCS-GFP and ACCS-M-GFP cells (5). Similarly, we continued our investigation by performing DNA microarray analysis using the ACCS-M-GFP and ACCS-LN-GFP cells, to uncover their differences at the molecular level. The results allowed us to comprehensively analyze the changes in ACCS-M-GFP and ACCS-LN-GFP gene expression, using 49,178 gene probes to search for metastasis-related genes in the two cell lines. A scatter plot of the signal values of ACCS-M-GFP and ACCS-LN-GFP gene expression showed the data with little dispersion and high reliability. Genetic differences were recognized when expression increased, with a Z-score ≥2.0 and a ratio ≥5.0, or when expression decreased, with a Z-score ≤-2.0 and a ratio of ≤0.2. We selected 20 up-regulated and 20 down-regulated candidate genes whose function is known (Figure 5).

Table I shows that NNMT expression was 2,000 times higher in ACCS-LN-GFP than in ACCS-M-GFP cells. Similarly, the expression of synaptic vesicle glycoprotein 2B (SV2B) was also enhanced, though to a lower extent. Contrarily, the expression of gap junction protein alpha-1 (GJA1) and of Defensin B3 was attenuated to 0.003-fold. The expression of N-cadherin, which is involved cell-cell

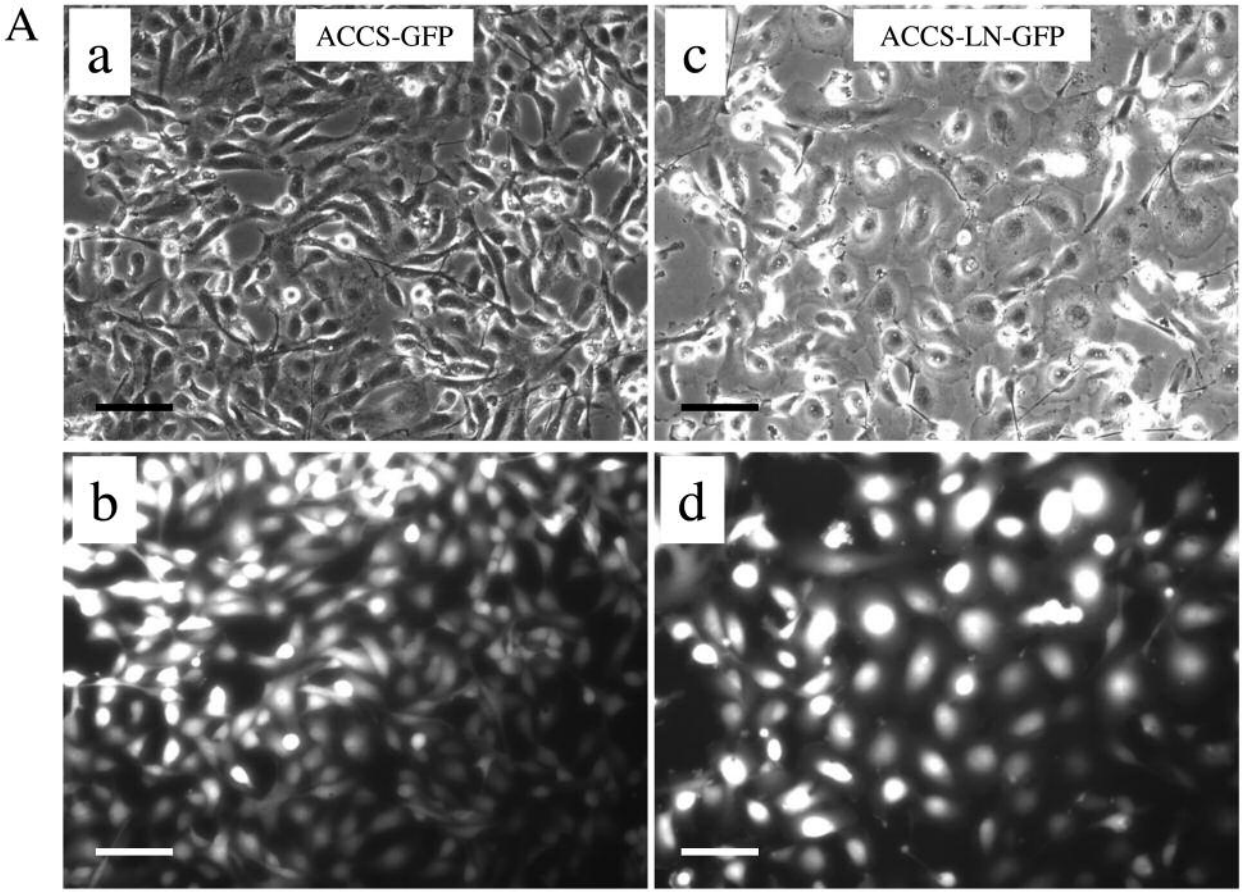

Figure 2. *Microscopic views of ACCS cell lines and the average of cell numbers per a field. (A) Cell morphology and GFP expression in the ACCS sub-lines. Phase-contrast (a and c) and fluorescence (b and d) images are shown. Scale bars indicate 100 μm. (B) Comparison of the number of the cells observed under the microscope. Each bar represents three independent experiments. *p<0.01.*

adhesion, was also attenuated in the ACCS-LN-GFP cells. No changes were observed in the expression of catenin or vimentin. Moreover, the expression of Brachyury, Snail and sex determining region Y-box 2 (SOX2), markers of cancer stem cells, did not significantly change (data not shown).

Changes in the expression of NNMT in the ACCS cell lines. The mRNA expression of *NNMT* in the ACCS cell lines was then investigated by qPCR. The expression level of *NNMT* in ACCS-LN-GFP cells was same as that of ACCS-M-GFP (Figure 6A). Then, we examined the protein levels of NNMT

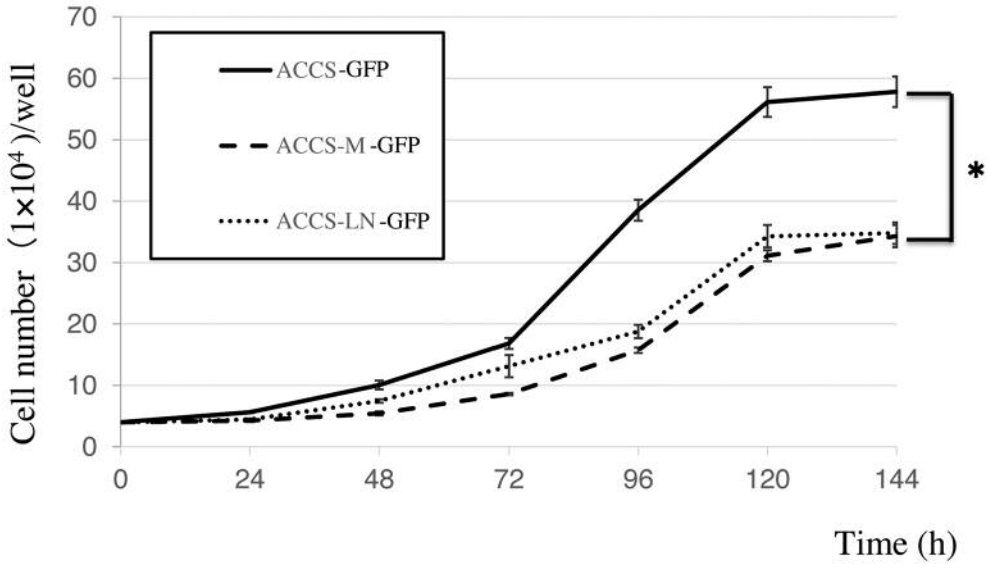

Figure 3. *Cell growth for the ACCS cell lines evaluated by cell count. Assays were performed in triplicate and repeated three times. Each point represents the mean of three independent experiments with standard error. *p<0.01.*

in our cell lines. ACCS-GFP cells expressed very low levels of NNMT, while the highly metastatic, and more so the lymph node metastatic cell lines, expressed higher NNMT levels (Figure 6B).

Discussion

AdCC is characterized by neural invasion and distant metastases, and shows low sensitivity to radiation and chemotherapy. Therefore, the effect of therapies is limited and the prognosis is generally poor (9, 10). We have previously studied the mechanism of invasion and metastasis in AdCC using *in vitro* AdCC invasion models (11, 12). However, metastasis is an intricate process that is difficult to mimic *in vitro*. Therefore, it was important to establish a spontaneous metastasis model for AdCC through orthotropic implantation. We previously established a highly-tumorigenic (ACCS-T-GFP) and a highly-metastatic (ACCS-M-GFP) cell line from the low-tumorigenicity cell line ACCS, using *in vivo* selection (5). These cell lines were polyclonal populations derived from the primary tumors. To identify metastasis-associated molecules, it is necessary to analyze the cells of the tumor metastases spontaneously originated. Published studies have investigated mechanism of metastasis in different kinds of carcinomas, through the injection of tumor cells into the mouse tail vein, and the subsequent establishment of metastatic cell lines (12, 13). However, these cell lines do not reflect key metastatic processes such as the detachment from the tumor site or the vascular invasion. Here, we generated a lymph node metastatic cell line (ACCS-LN-GFP) from ACCS cells. The present study is one of the few reports that established a cell line from metastatic tissue, isolated thanks to the fluorescence of the GFP the metastatic cells expressed (14, 15). Because of the way these cell lines were generated, they most likely represent a monoclonal cell population.

We compared the parental, the highly-metastatic cells and the lymph node metastatic cells. First, we examined the characteristics of the cell line generated. The proliferation of the cells with high metastatic potential was reduced compared to that of the parental cell line. However, their migration ability increased. This phenomenon is consistent with clinical observations in patients with AdCC.

We have reported that ACCS-M-GFP cells have a strong sphere-forming ability compared to ACCS-GFP cells (6). Similarly, the ACCS-LN-GFP cell line that we generated exhibited strong colonization capabilities, suggesting that ACCS-LN-GFP cells might have characteristics of CSC (data not shown).

In DNA microarray analysis, we compared the expression of markers of CSC such as Brachyury, Oct-4, SOX2, Snail, Slug and Twist in ACCS-M-GFP and ACCS-LN-GFP. The expression of these markers did not significantly change in the two cell lines. This observation does not deny the CSC potential of the ACCS-LN-GFP cells. We believe we did not find changes in the expression of CSC-related genes because ACCS-LN-GFP cells derive from ACCS-M-GFP cells, which, being metastatic, might already possess CSC features.

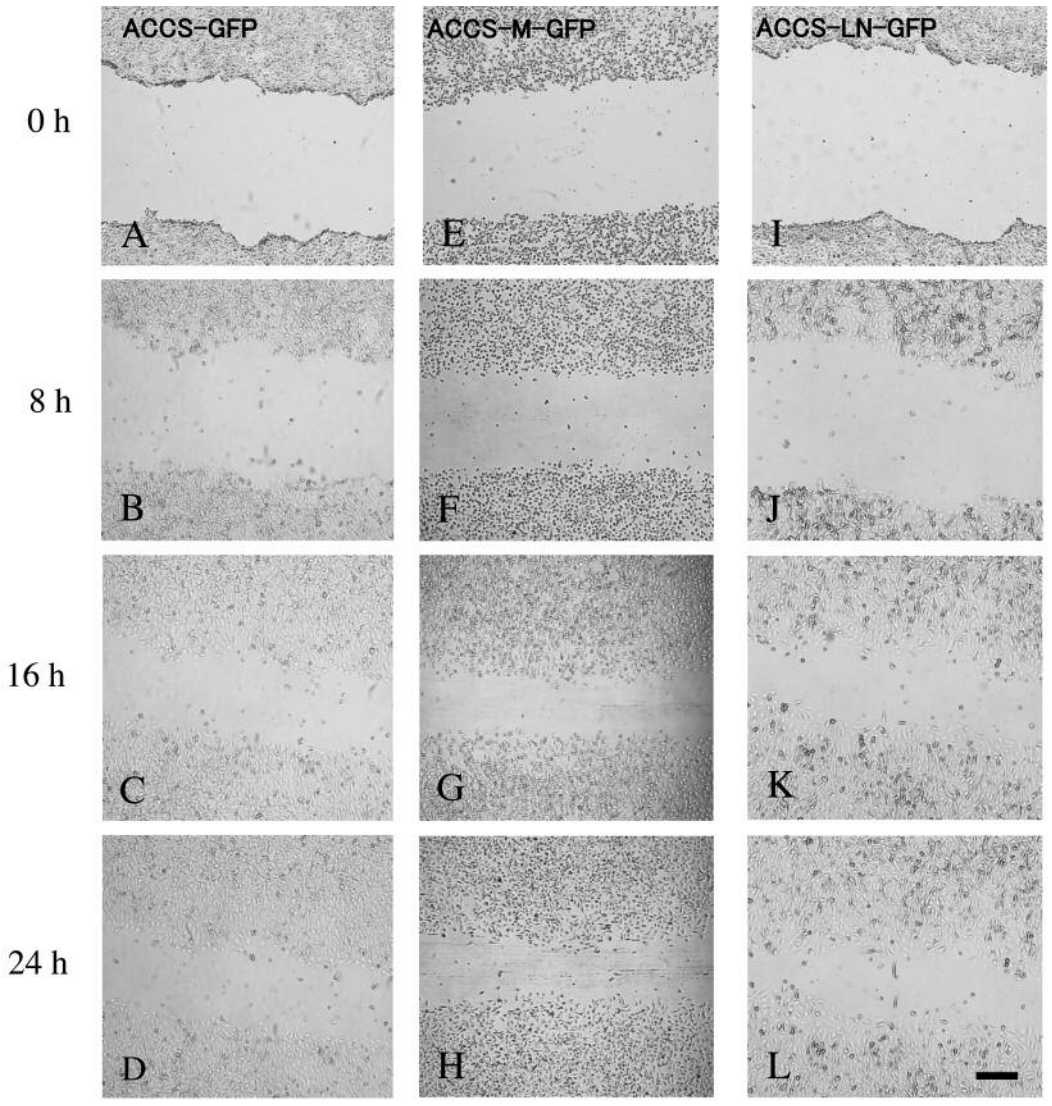

Figure 4. *Cell migration in the ACCS cell lines. Migration was evaluated by using a wound-healing assay, as described in Materials and Methods. The wound regions were photographed 24 h after the start of the assay (A, E, I: 0 h; B, F, J: 8 h; C, G, K: 16 h; D, H, L: 24 h). (A-D) ACCS-GFP, (E-H) ACCS-M-GFP, (I-L) ACCS-LN-GFP. Data significance was analyzed using the Student's t-test: no significant differences were found.*

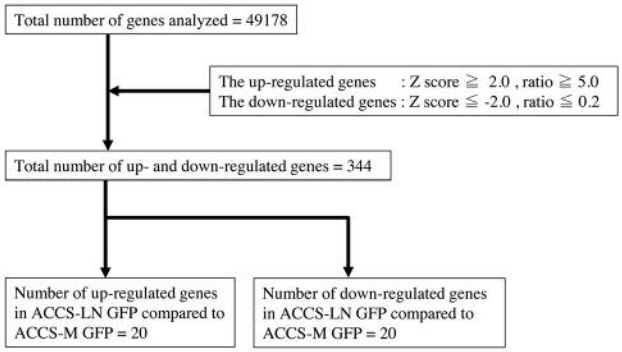

Figure 5. *Screening of significant genes for cancer and metastasis. The 49,178 genes were filtered as indicated. Twenty up-regulated and 20 down-regulated candidate genes related to cancer or metastasis, and whose functions is known, were selected.*

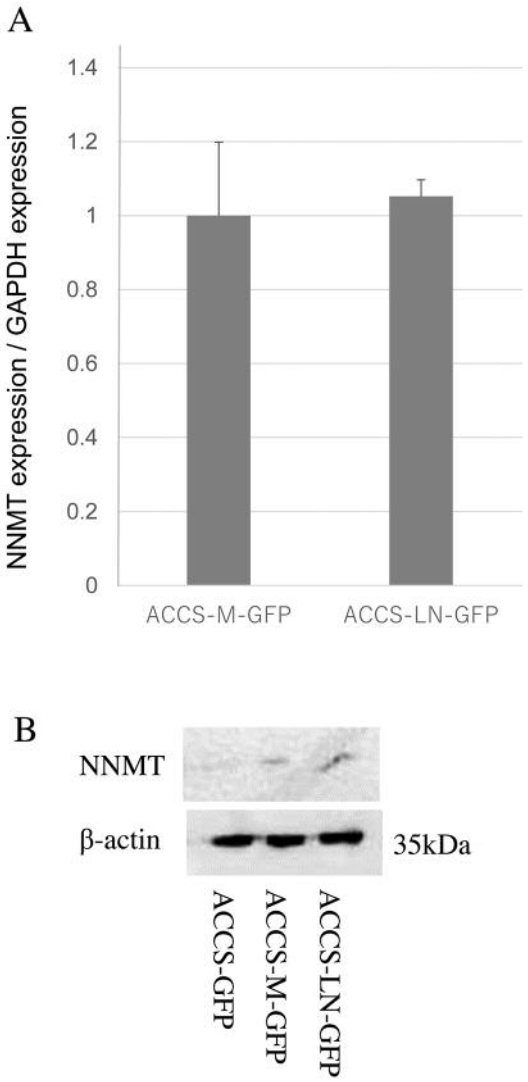

Figure 6. *mRNA and protein levels of NNMT. (A) Relative levels of mRNA related to various regulatory B subunits in ACCS-M-GFP and ACCS-LN-GFP cells, as determined by qPCR. Each bar represents the mean of five independent experiments with the standard error. (B) Lymph node metastatic cells show increased expression of NNMT compared to the parental ACCS-M-GFP and ACCS-GFP cells. All ACCS cells were cultured for 24 h on culture dishes, prior to protein extraction. This experiment was performed in triplicate, and representative results are shown.*

Decreased cell adhesion plays an important role in tumor metastasis. Our microarray data revealed the variation of fewer cell adhesion-related molecules than we expected. Among these, GJA1 was markedly down-regulated in ACCS-LN-GFP. Gap junctions are membrane channels composed of proteins called connexins. GJA1, also called connexin 43, is the most ubiquitously expressed connexin (16) and is considered a tumor suppressor for its role in reversing the phenotype of cancer cells (17, 18). Decreased expression of connexin 43 remarkably diminishes the number of gap junctions, promoting cancer metastatic dissemination (19).

We also reported the loss of E-cadherin and integrins and the gain of vimentin in ACCS-M-GFP cells; this phenomenon suggested that the EMT is a putative event in AdCC metastasis (5). In the current study, the protein whose expression was changed the most in ACCS-LN-GFP cells was NNMT. NNMT is a recently identified potential tumor biomarker; it is a phase II metabolizing enzyme that catalyzes the N-methylation of nicotinamide, pyridines, and other structural analogs involved in the biotic formation and in the detoxification of a number of xenobiotics (20, 21). Several studies have found that NNMT mRNA and protein levels are up-regulated and correlate with poor prognosis in several tumors including oral squamous cell carcinoma (22), renal cell cancer (23), lung cancer (24), prostate cancer (25), gastric carcinoma (26), and pancreatic cancer (27). In these studies, the expression of NNMT in cancerous tissues was higher than that in corresponding non-cancerous tissues. Moreover, the levels of NNMT correlated with tumor size, lymph node metastasis, distant metastasis, and overall survival. Furthermore, NNMT expression positively correlated with the phosphorylation of Akt, and negatively associated with disease-free survival and local recurrence-free survival (28). NNMT affects tumorigenesis because it impairs the methylation potential of cancer cells by consuming methyl units from S-adenosylmethionine to create the stable metabolic product 1-methylnicotinamide. As a result, NNMT-expressing cancer cells possess an altered epigenetic state that includes hypomethylated histones and other cancer-related proteins, combined with heightened

Table I. *The 20 most significant up- and down-regulated genes in lymph node metastatic ACCS-LN-GFP cells.*

A. Up-regulated genes

	ProbeID	GeneSymbol	GeneID	Description	Ratio	Z score
1	A_23_P127584	*NNMT*	4837	Nicotinamide N-methyltransferase	2190.9	19.61
2	A_23_P100022	*SV2B*	9899	Synaptic vesicle glycoprotein 2B	226.2	9.59
3	A_23_P205164	*POU4F1*	5457	POU class 4 homeobox 1	110.2	8.32
4	A_33_P3228622	*OR14I1*	401994	Olfactory receptor, family 14, subfamily I, member 1	100.7	8.16
5	A_24_P911906	*PCDH17*	27253	Protocadherin 17	48.9	3.47
6	A_33_P3300747	*ADHFE1*	137872	Alcohol dehydrogenase, iron containing, 1	30.9	6.07
7	A_33_P3399150	*ORAOV1*	220064	Oral cancer overexpressed 1	28.6	3.00
8	A_32_P140489	*GDF6*	392255	Growth differentiation factor 6	28.5	3.00
9	A_24_P189997	*PCSK6*	5046	Proprotein convertase subtilisin/kexin type 6	28.0	2.98
10	A_21_P0007483	*SSPN*	8082	Sarcospan	27.3	2.96
11	A_33_P3292769	*NFAM1*	150372	NFAT activating protein with ITAM motif 1	26.8	2.95
12	A_33_P3249224	*BAAT*	570	Bile acid CoA:amino acid N-acyltransferase	25.5	2.90
13	A_23_P258136	*MXRA5*	25878	Matrix-remodelling associated 5	24.2	2.86
14	A_32_P234518	*AWAT1*	158833	Acyl-CoA wax alcohol acyltransferase 1	24.0	2.85
15	A_23_P49759	*CCL1*	6346	Chemokine (C-C motif) ligand 1	23.1	2.82
16	A_33_P3348569	*OR9G4*	283189	Olfactory receptor, family 9, subfamily G, member 4	21.3	2.75
17	A_19_P00315922	*WDFY4*	57705	WDFY family member 4	20.1	2.70
18	A_23_P103703	*HSPB7*	27129	Heat shock protein family, member 7	18.4	2.62
19	A_33_P3384287	*PALM*	5064	Paralemmin	17.6	9.63
20	A_33_P3687198	*HRK*	8739	Harakiri, BCL2 interacting protein	17.2	2.56

B. Down-regulated genes

	ProbeID	GeneSymbol	GeneID	Description	Ratio	Z score
1	A_33_P3377090	*GJA1*	2697	Gap junction protein, alpha 1	0.0031	–14.73
2	A_23_P169017	*DEFB103B*	55894	Defensin, beta 103B	0.0037	–14.28
3	A_33_P3241269	*CES1*	1066	Carboxylesterase 1	0.0049	–9.43
4	A_33_P3332150	*APOBEC4*	403314	Apolipoprotein B mRNA editing enzyme, Catalytic polypeptide-like 4	0.0090	–8.35
5	A_33_P3260430	*SPRR2A*	6700	Small proline-rich protein 2A	0.0097	–8.22
6	A_23_P161698	*MMP3*	4314	Matrix metallopeptidase 3	0.0103	–11.66
7	A_23_P210465	*PI3*	5266	Peptidase inhibitor 3	0.0112	–11.46
8	A_24_P190472	*SLPI*	6590	Secretory leukocyte peptidase inhibitor	0.0125	–11.18
9	A_24_P381199	*TRIM6*	117854	Tripartite motif containing 6	0.0156	–7.37
10	A_24_P58204	*OR51B5*	282763	Olfactory receptor, family 51, subfamily B, member 5	0.0176	–7.15
11	A_23_P1691	*MMP1*	4312	Matrix metallopeptidase 1	0.0196	–6.96
12	A_23_P2181	*CYB5R2*	51700	Cytochrome b5 reductase 2	0.0238	–3.19
13	A_33_P3226761	*SOX18*	54345	SRY (sex determining region Y)-box 18	0.0250	–6.54
14	A_23_P253536	*NPR3*	4883	Natriuretic peptide receptor 3	0.0265	–3.09
15	A_19_P00811828	*ZNF737*	100129842	Zinc finger protein 737	0.0269	–3.08
16	A_23_P129005	*NYNRIN*	57523	NYN domain and retroviral integrase containing	0.0274	–6.38
17	A_23_P117851	*CPLX3*	594855	Complexin 3	0.0283	–3.04
18	A_23_P217379	*COL4A6*	1288	Collagen, type IV, alpha 6	0.0292	–9.02
19	A_23_P64919	*RERGL*	79785	RERG/RAS-like	0.0383	–2.77
20	A_23_P11644	*SPRR2D*	6703	Small proline-rich protein 2D	0.0411	–5.66

expression of pro-tumorigenic gene products (29). Our data showed that the expression of NNMT enhanced tumor malignancy; in fact, the expression of NNMT increased from the low tumorigenic ACCS cell line to the highly-metastatic ACCS-M-GFP and lymph node metastasis ACCS-LN-GFP cell lines. These results suggest that NNMT might be a novel biomarker for malignancy. Accordingly, silencing of NNMT is associated to decreased cell proliferation and colony formation *in vitro*, and induces a marked reduction in tumor volume *in vivo* (30-32). These results suggest that inhibition of NNMT could represent a potential molecular approach for the treatment of malignant diseases.

Some studies have found that NNMT is highly expressed in CSC (33, 34). As noted above, ACCS-LN-GFP cells might have CSC features, including the up-regulation of NNMT and the loss of GJA1, which lead to the EMT and consequent AdCC metastasis.

Recent reports indicate that NNMT can be detected in serum (35, 36), urine (37) and saliva (38), suggesting its usefulness as a diagnostic tool for AdCC and metastatic tumors in general. Importantly, recent studies indicate the microRNA in the serum may be useful for diagnosis or gene target therapy (39, 40). Hui *et al*. reported that NNMT levels correlate with the expression of microRNA-1291 in pancreatic carcinoma cells (41) and suggest that NNMT might be a marker of pancreatic carcinogenesis. Similarly, NNMT could serve as a biomarker for adenoid cystic carcinoma. Further studies are necessary to fully evaluate if NNMT can be used as a novel and effective tumor biomarker.

Conflicts of Interest

The Authors declare no financial or other potential conflict of interest in regard to this study.

Acknowledgements

This work was supported by JSPS KAKENHI Grant Number GAG5K20540 and 15K11257. The Authors gratefully acknowledge this financial support. The Authors would also like to thank Editage for English language editing.

References

1 Rapidis AD, Givalos N, Gakiopoulou H, Faratzis G, Stavrianos SD, Vilos GA, Douzinas EE and Patsouris E: Adenoid cystic carcinoma of the head and neck. Clinicopathological analysis of 23 patients and review of the literature. Oral Oncol *41*: 328-335, 2005.

2 Ampil FL and Misra RP: Factors influencing survival of patients with adenoid cystic carcinoma of the salivary glands. J Oral Maxillofac Surg *45*: 1005-1010, 1987.

3 Kobayashi Y, Sugiura T, Imajyo I, Shimoda M, Ishii K, Akimoto N, Yoshihama N and Mori Y: Knockdown of the T-box transcription factor Brachyury increases sensitivity of adenoid cystic carcinoma cells to chemotherapy and radiation *in vitro*: Implications for a new therapeutic principle. Int J Oncol *44*: 1107-1117, 2014.

4 Hitre E, Budai B, Takácsi-Nagy Z, Rubovszky G, Tóth E, Remenár É, Polgár C and Láng I: Cetuximab and platinum-based chemoradio- or chemotherapy of patients with epidermal growth factor receptor expressing adenoid cystic carcinoma: a phase II trial. Br J Cancer *109*: 1117-1122, 2013.

5 Ishii K, Shimoda M, Sugiura T, Seki K, Takahashi M, Abe M, Matsuki R, Inoue Y and Shirasuna K: Involvement of epithelial-mesenchymal transition in adenoid cystic carcinoma metastasis. Int J Oncol *38*: 921-931, 2011.

6 Shimoda M, Sugiura T, Imajyo I, Ishii K, Chigita S, Seki K, Kobayashi Y and Shirasuna K: The T-box transcription factor Brachyury regulates epithelia-mesenchymal transitions in association with cancer stem-like cells in adenoid cystic carcinoma cells. BMC Cancer *12*: 377, 2012.

7 Herrmann BG, Labeit S, Poustka A, King TR and Lehrach H: Cloning of the T gene required in mesoderm formation in the mouse. Nature *343*: 617-622, 1990.

8 hirasuna K, Watatani K, Furusawa H, Saka M, Morioka S, Yoshioka H and Matsuya T: Biological characterization of pseudocyst-forming cell lines from human adenoid cystic carcinomas of minor salivary gland origin. Cancer Res *50*: 4139-4145, 1990.

9 Ko JJ, Siever JE, Hao D, Simpson R, Lau HY: Adenoid cystic carcinoma of head and neck: clinical predictors of outcome from a Canadian centre. Curr Oncol *23*: 26-33, 2016.

10 Ouyang DQ, Liang LZ, Zheng GS, Ke ZF, Weng DS, Yang WF, Su YX and Liao GQ: Risk factors and prognosis for salivary gland adenoid cystic carcinoma in southern china: A 25-year retrospective study Medicine (Baltimore) *96*: e5964, 2017.

11 Abu-Ali S, Sugiura T, Takahashi M, Shiratsuchi T, Ikari T, Seki K, Hiraki A, Matsuki R and Shirasuna K: Expression of the urokinase receptor regulates focal adhesion assembly and cell migration in adenoid cystic carcinoma cells. J Cell Physiol *203*: 410-419, 2005.

12 Seki K, Ishii K, Sugiura T, Takahashi M, Inoue Y and Shirasuna K: An adenoid cystic carcinoma cell line possessing high metastatic activity has high NF-κB activation in response to TNF-α. Oral Sci Int *2*: 36-44, 2005.

13 Kuwabara Y, Yamada T, Yamada, Yamazaki K, Du WL, Kouji B, Aoki D and Sakamoto M: Establishment of an ovarian metastasis model and possible involvement of E-cadherin down-regulation in the metastasis. Cancer Sci *9*: 1933-1939, 2008.

14 Su Y, Luo X, He BC, Wang Y, Chen L, Zuo GW, Liu B, Bi Y, Huang J, Zhu GH, He Y, Kang Q, Luo J, Shen J, Chen J, Jin X, Haydon RC, He TC and Luu HH: Establishment and characterization of a new highly metastatic human osteosarcoma cell line Clin Exp Metastasis *26*: 599-610, 2009.

15 Eckhardt BL, Parker BS, van Laar RK, Restall CM, Natoli AL, Tavaria MD, Stanley KL, Sloan EK, Moseley JM and Anderson RL: Genomic analysis of a spontaneous model of breast cancer metastasis to 950 bone reveals a role for the extracellular matrix. Mol Cancer Res *3*: 1-13, 2005.

16 Goodenough DA, Goliger JA and Paul DL: Connexins, Connexons, and intercellular communication (Review) Ann Rev Biochem *65*: 475-502, 1996.

17 Tittarelli A, Guerrero I, Tempio F, Gleisner MA, Avalos I, Sabanegh S, Ortíz C, Michea L, López MN, Mendoza-Naranjo A and Salazar-Onfray F: Overexpression of connexin 43 reduces melanoma proliferative and metastatic capacity. Br J Cancer *113*: 259-267, 2015.

18 Zhang A, Hitomi M, Bar-Shain N, Dalimov Z, Ellis L, Velpula KK, Fraizer GC, Gourdie RG and Lathia JD: Connexin 43 expression is associated with increased malignancy in prostate cancer cell lines and functions to promote migration. Oncotarget. *6*: 11640-11651, 2015.

19 Mao XY, Li QQ, Gao YF, Zhou HH, Liu ZQ and Jin WL: Gap junction as an intercellular glue: Emerging roles in cancer EMT and metastasis. Cancer Lett *381*: 133-137, 2016.

20 Aksoy S, Szumlanski CL and Weinshilboum RM: Human liver nicotinamide N-methyltransferase. J Bio Chem *269*: 14835-14840, 1994.

21 Hong S, Moreno-Navarrete JM, Wei X, Kikukawa Y, Tzameli I, Prasad D, Lee Y, Asara JM, Fernandez-Real JM, Maratos-Flier E and Pissios P: Nicotinamide N-methyltransferase regulates hepatic nutrient metabolism through Sirt1 protein stabilization. Nat Med *21*: 887-894, 2015.
22 Sartini D, Santarelli A, Rossi V, Goteri G, Rubini C, Ciavarella D, Muzio L and Emanuelli M: Nicotinamide N-methyltransferase upregulation inversely correlates with lymph node metastasis in oral squamous cell carcinoma. Mol Med *13*: 415-421, 2007.
23 Zhang J, Xie XY, Yang SW, Wang J and He C: Nicotinamide N-methyltransferase protein expression in renal cell cancer. J Zhejiang Univ Sci B *11*: 136-143, 2010.
24 Sartini D, Morganti S, Guidi E, Rubini C, Zizzi A: Nicotinamide N-methyltransferase in non-small cell lung cancer: Promising results for targeted anti-cancer therapy. Cell Biochem Biophys *67*: 865-873, 2013.
25 Zhou W, Gui M, Zhu M, Long Z, Huang L, Zhou J, He L and Zhong L: Nicotinamide N methyltransferase is overexpressed in prostate cancer and correlates with prolonged progression free and overall survival time. Oncol Lett *8*: 1175-1180, 2014.
26 Chen C, Wang X, Huang X, Yong H, Shen J, Tang Q, Zhu J, Ni J and Feng Z. Nicotinamide N-methyltransferase: a potential biomarker for worse prognosis in gastric carcinoma. Am J Cancer Res *6*: 649-663, 2016.
27 Xu Y, Liu P, Zheng DH, Wu N, Zhu L, Xing C and Zhu J: Expression profile and prognostic value of NNMT in patients with pancreatic cancer Oncotarget *7*: 19975-19981, 2016.
28 Win KT, Lee SW, Huang HY, Lin LC, Lin CY, Hsing CH, Chen LT and Li CF: Nicotinamide N-methyltransferase overexpression is associated with Akt phosphorylation and indicates worse prognosis in patients with nasopharyngeal carcinoma. Tumour Bio *34*: 3923-3931, 2013.
29 Ulanovskaya OA, Zuhl AM, and Cravatt BF: NNMT promotes epigenetic remodeling in cancer by creating a metabolic methylation sink. Nat Chem Biol *9*: 300-306, 2013.
30 Sartini D, Seta R, Pozzi V, Morganti S, Rubini C, Zizzi A, Tomasetti M, Santarelli L and Emanuelli M: Role of nicotinamide N-methyltransferase in non-small cell lung cancer: *in vitro* effect of shRNA-mediated gene silencing on tumourigenicity. Biol Chem *396*: 225-234, 2015.
31 Pozzi V, Sartini D, Morganti S, Giuliante R, Di Ruscio G, Santarelli A, Rocchetti R, Rubini C, Tomasetti M, Giannatempo G, Orlando F, Provinciali M, Lo Muzio L and Emanuelli M: RNA-mediated gene silencing of nicotinamide N-methyltransferase is associated with decreased tumorigenicity in human oral carcinoma cells. PLoS One *8*: e71272, 2013.
32 Pozzi V, Mazzotta M, Lo Muzio L, Sartini D, Santarelli A, Renzi E, Rocchetti R, Tomasetti M, Ciavarella D and Emanuelli M: Inhibiting proliferation in KB cancer cells by RNA interference-mediated knockdown of nicotinamide N-methyltransferase. Int J Immunopathol Pharmacol *24*: 69-77, 2011.
33 Pozzi V, Sartini D, Rocchetti R, Santarelli A, Rubini C, Morganti S, Giuliante R, Calabrese S, Di Ruscio G, Orlando F, Provinciali M, Saccucci F, Lo Muzio L and Emanuelli M: Identification and characterization of cancer stem cells from head and neck squamous cell carcinoma cell lines. Cell Physiol Biochem *36*: 784-798, 2015.
34 D'Andrea FP, Safwat A, Kassem M, Gautier L, Overgaard J and Horsman MR: Cancer stem cell overexpression of nicotinamide N-methyltransferase enhances cellular radiation resistance. Radiother Oncol *99*: 373-378, 2011.
35 Tomida M, Mikami I, Takeuchi S, Nishimura H, Akiyama H: Serum levels of nicotinamide N-methyltransferase in patients with lung cancer. J Cancer Res Clin Oncol *135*: 1223-1229, 2009.
36 Roessler M, Rollinger W, Palme S, Hagmann ML, Berndt P, Engel AM, Schneidinger B, Pfeffer M, Andres H, Karl J, Bodenmüller H, Rüschoff J, Henkel T, Rohr G, Rossol S, Rösch W, Langen H, Zolg W and Tacke M: Identification of nicotinamide N-methyltransferase as a novel serum tumor marker for colorectal cancer. Clin Cancer Res *11*: 6550-6557, 2005.
37 Sartini D, Muzzonigro G, Milanese G, Pozzi V, Vici A, Morganti S, Rossi V, Mazzucchelli R, Montironi R and Emanuelli M: Upregulation of tissue and urinary nicotinamide n-methyltransferase in bladder cancer: Potential for the development of a urine-based diagnostic test cell. biochem biophys *65*: 473-483, 2013.
38 Pozzi V, Sartini D, Morganti S, Giuliante R, Di Ruscio G, Santarelli A, Rocchetti R, Rubini C, Tomasetti M, Giannatempo G, Orlando F, Provinciali M, Lo Muzio L and Emanuelli M: RNA-Mediated gene silencing of nicotinamide N-methyltransferase is associated with decreased tumorigenicity in human oral carcinoma cells. PLoS One *8*: e71272, 2013.
39 Mine M, Yamaguchi K, Sugiura T, Chigita S, Yoshihama N, Yoshihama R, Hiyake N, Kobayashi Y and Mori Y: miR-203 Inhibits Frizzled-2 Expression *via* CD82/KAI1 Expression in Human Lung Carcinoma Cell.s PLoS One 10: e0131350, 2015.
40 Iorio MV and Croce CM: MicroRNA dysregulation in cancer: diagnostics, monitoring and therapeutics. A comprehensive review. EMBO Mol Med *4*: 143-159, 2012.
41 Bi HC, Pan YZ, Qiu JX, Krausz KW, Li F, Johnson CH, Jiang CT, Gonzalez FJ and Yu AM: N-methylnicotinamide and nicotinamide N-methyltransferase are associated with microRNA-1291-altered pancreatic carcinoma cell metabolome and suppressed tumorigenesis. Carcinogenesis *35*: 2264-2272, 2014.

Received October 6, 2017
Revised October 22, 2017
Accepted October 23, 2017